MEASUREMENT OF THERMAL CONDUCTIVITY AND VOLUMETRIC HEAT CAPACITY AS A FUNCTION OF HUMIDITY AND TEMPERATURE USING A SINGLE HEATED WIRE

Victor A. Băileșteanu(s2844230)
Supervisors: Dr. Remco J. Wiegerink, M.Sc. Shirin Azadi Kenari

ABSTRACT

A flow-independent gas property meter was developed to analyse two thermal properties of a gas, namely the thermal conductivity (k) and the volumetric heat capacity (ρc_p). The sensor will be used to calibrate a gas flow sensor accordingly for the present gas. This paper shows how the two properties are influenced by ambient temperature and relative humidity in the case of air. The literature presents contradictory results. The experimental findings of this paper show that the ambient temperature has a considerable influence on thermal conductivity while the humidity plays a minor role. The volumetric heat capacity measurements were inconclusive and further research is required to understand the effects of ambient temperature and relative humidity on it.

Keywords - volumetric heat capacity, thermal conductivity,* 3ω *method, humid air, temperature dependency

1 INTRODUCTION

Gas flow sensors are widely used in various domains. However, the gas needs to be identified by two of its properties before assessing the flow of the gas, i.e. the thermal conductivity (k) and the volumetric heat capacity (ρc_p). The existing flow sensors are manufactured to detect the flow of a certain gas or gas mixture, e.g. air, and require calibration if a new gas is present. A novel sensor that can detect the gas by analysing the two mentioned properties, and then determine the flow was developed at the IDS Group of the University of Twente [1].

The gas detection sensor consists of a suspended wire that is operated using two different measurement methods to identify both properties, a DC measurement for the thermal conductivity and an AC one for the volumetric heat capacity. It is known that the resistance of a wire is directly proportional to the ambient temperature. Moreover, there is a chance that the relative humidity of the gas can affect the parameters. Therefore, this paper presents an investigation of the effect of temperature and relative humidity on air's thermal conductivity and volumetric heat capacity.

2 SENSOR DESIGN AND WORKING PRINCIPLE

The sensor is a platinum hot wire placed on a beam and suspended over a V-groove. The wire is a resistor that is heated by a current. Its temperature depends on the heat conducted through the gas from the wire to the substrate. The role of the V-groove is to form a volume between the platinum wire and the silicon substrate that will facilitate a thermal resistance effect which changes with the thermal conductivity of the gas present in the volume [1]. A photograph of the groove and wire made with a microscope can be seen in Figure 1. The sensor is situated perpendicular to the flow and

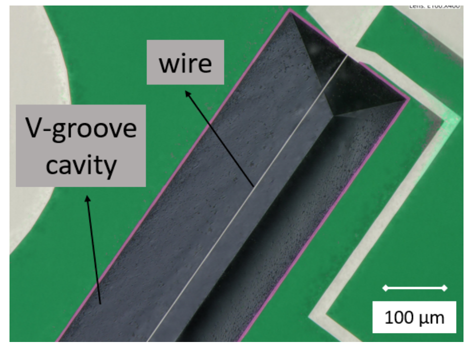

Figure 1: Microscope photograph of the sensor. Image taken from [2].

close to the wall of the tube in which it will be inserted to cancel the effect of the flow on the measurement. Due to the groove's shape, it is uncertain how much of the heat will be conducted to the substrate, but it is assumed that the effective distance from the wire to the substrate is approximately half of the V-groove's depth. The volume around the wire will facilitate a thermal capacitive effect, but it is uncertain what the shape and how large it is. Figure 2 shows a cross-sectional drawing of the sensor.

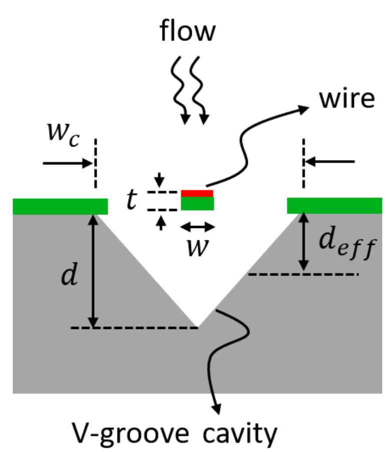

Figure 2: Cross-sectional drawing of the sensor. Image taken from [2].

Another uncertainty is the actual relative humidity in the V-groove since the temperature around the wire is higher than the one in the environment and the humidity percentage might decrease.

2.1 Thermal conductivity

The equation that defines the dependency of resistance on the temperature of the resistor is:

$$\begin{aligned} R &= R_0(1+\alpha(T-T_0)) \\ &= R_0 + m(T-T_0) \end{aligned} \tag{1}$$

where R_0 is the resistance at wire temperature T_0, α is platinum's temperature coefficient of resistance, R is the resistance at wire temperature T and m=αR_0 is the slope that defines the resistance's dependency on temperature. Two different sets of R_0 and T_0 can be used in the equation.

The first set contains the values of the resistance of the unheated wire, i.e. when a low DC current ($\leq$200 μA) is applied, at the same temperature and relative humidity as the ones of the heated wire, i.e. when a higher DC current ($\geq$1 mA) is applied. The second uses a fixed R_0 for the unheated wire, i.e. the one corresponding to 0 °C. It was discovered that the second is more reliable and it will be used in this study.

$$R_{\text{heated}} = R_{\text{unheated},0^\circ\text{C}} + m \cdot (T_{\text{wire}} - 0) \tag{2}$$

The temperature difference between the wire and ambient temperature, $\Delta T = T_{\text{wire}} - T_{\text{ambient}}$, can be calculated and used in the thermistor's equation to calculate the thermal conductivity. The thermistor (R_{th}) is characterised by the following equation:

$$\Delta T = P \cdot R_{\text{th}} = R_{\text{heated}} \cdot I^2 \cdot \frac{d_{\text{eff}}}{k \cdot A} \tag{3}$$

where d_{eff} and A are the effective depth of the V-groove and its area seen from above, R is the resistance of the wire, I is the current flowing through it and k is the thermal conductivity of the surrounding gas. Rewriting Equation (3) to calculate k yields the following result:

$$k = \frac{R_{\text{heated}} \cdot I^2 \cdot d_{\text{eff}}}{\Delta T \cdot A} \tag{4}$$

2.2 Volumetric heat capacity

The volumetric heat capacity is measured using the same wire as in the thermal conductivity acquisition experiment. However, alternating current is applied to it instead of DC because ρc_p can be obtained using the voltage amplitude of the third harmonic, hence the name of the "3ω method". The second harmonic influences the power and will result in changes in the wire temperature and resistance. This will lead to the third harmonic's high dependency on the ambient gas' properties [2]. Equation (5) shows the amplitude of the third harmonic. The full derivation can be found in [2].

$$|V_{3\omega}| = \frac{I_{\text{ac}}^3 R_{\text{heated}} R_0 \alpha}{4} |Z_{2\omega}| \tag{5}$$

3 THERMAL CONDUCTIVITY

3.1 Literature review

Various research papers show different results regarding the effect of relative humidity (RH) on the air's thermal conductivity. Emperhoff et al. [3] report that by using three different sensors they observed a rise in thermal conductivity for RH levels between 0% and 50% followed by a decrease for higher humidity levels at a fixed ambient temperature, while also mentioning the work of multiple researchers, namely Tsilingiris [4] and Pernau et al. [5], that proved the intuitive answer, i.e. the thermal conductivity only decreases as more water vapour is added to the system since the water vapour's k is smaller than the one of dry air.

However, Boukhriss et al. [6] showed that as the humidity increases the thermal conductivity becomes higher. Wu et al. [7] showed that Boukhriss' values can be described by fourth-order polynomials. Tsilingiris also revealed that the thermal conductivity is defined by fourth-order polynomials for different relative humidities, but after certain temperatures, the thermal conductivity presents a drop in value [4]. Figure 3 shows Wu's and Boukhriss' findings, as presented by Wu et al. [7].

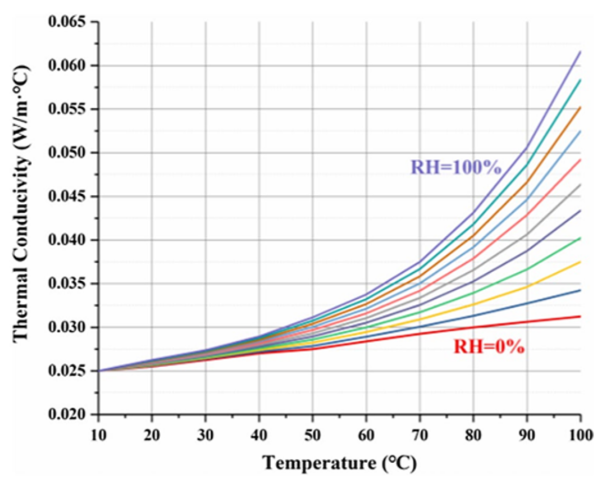

Figure 3: Thermal conductivity as a function of ambient temperature for various relative humidity. Image taken from [7].

3.2 Experimental setup

The sensor is placed in a Hettich PRC 1200 WL cabinet, i.e. a climate chamber that can change the interior temperature and relative humidity, and connected to a Keithley 2410 Source Measure Unit that supplies a direct current and reads the wire's voltage. The cabinet can fail to provide and measure correctly the temperature and relative humidity, therefore an auxiliary Dracal PTH450 temperature, humidity and pressure sensor was placed in the chamber as close as possible to the gas identification sensor. The two data acquisition devices are connected to a computer that runs a Labview program storing the data in a comma-separated file, i.e. the supplied current and the measured voltage, used to calculate the wire's resistance, the ambient temperature and the relative humidity.

The acquired data was processed in Matlab to analyse the influence of temperature and humidity on the resistance and, subsequently, on the thermal conductivity. Two experiments using the same air conditions, i.e. temperature increases from 25 °C to 50 °C in steps of 5 °C for a relative humidity of 30, 50, 70, and 90% at approx. 101.7 kPa, were conducted. One monitors the voltage across the wire in these conditions when a small 100 μA DC, not enough to result in self-heating, is applied to it and the other when the 2 mA DC that induces a self heating effect is supplied. The climate chamber allows the user to set a program by fixing temperature and humidity setpoints and time length for the ramp between each step and the ones of the steps. To ensure that the tested sensor reaches the same temperature as the one read by the commercial sensor, the time allotted for each step was selected as 3 hours, while the ramp was chosen as 10 minutes.

3.3 Findings

It is believed that the relative humidity will not impact the resistance when a DC of 100 μA flows through the wire. The following experiment shows the resistance of the wire sensor changing with the ambient temperature while the relative humidity is fixed at 90%($\pm$5%). The unheated wire resistance and the ambient temperature are plotted as functions of time in Figure 4.

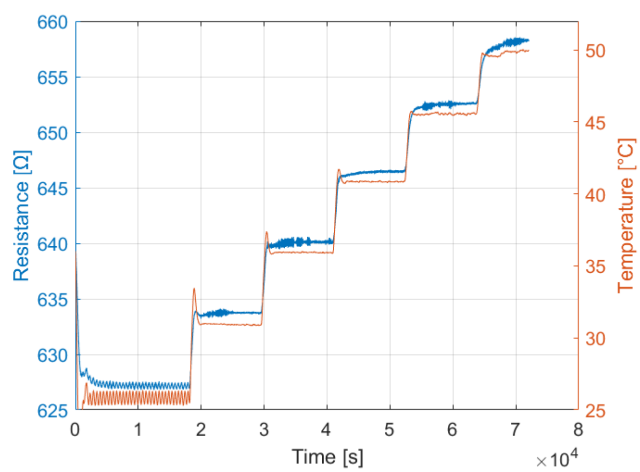

Figure 4: Resistance and temperature as functions of time when a current of 100 μA is applied.

From Figure 4, it can be concluded that the resistance is highly dependent on the ambient temperature, with both graphs having a very similar shape. It can also be seen that the resistance reaches the steady state after a longer period than the temperature measurement of the Dracal sensor, i.e. almost two hours, due to the large volume of the climate chamber. For each step, the average temperature and resistance in the steady state were calculated and used to obtain a linear equation for the resistance as a function of ambient temperature. The values are not perfectly linear, but a first-order polynomial was used in Matlab to obtain Equation (6) which is based on Equation (2).

$$R_{\text{unheated}} = c_1 + c_2 \cdot T_{\text{ambient}} \tag{6}$$

where c_1 = 593.932 Ω is the resistance of the unheated wire at 0 °C and c_2 = 1.2867 $\Omega/°$C is the slope that defines the linear increase of the resistance with the ambient temperature.

Figure 5 shows the experimental values and the first-order polynomial fit obtained using them.

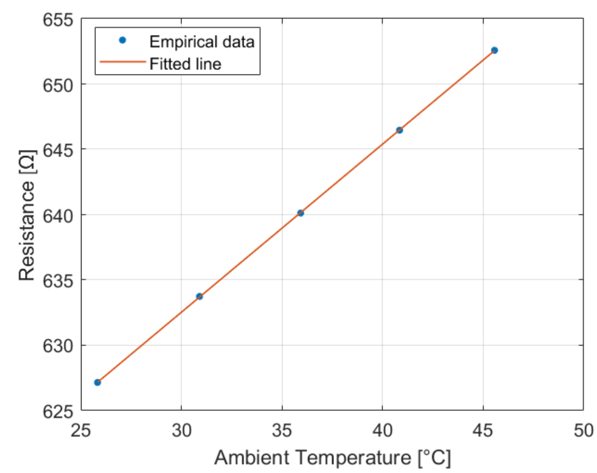

Figure 5: Acquired unheated wire resistance and the fitted line plot as functions of ambient temperature.

The same behaviour with respect to the ambient temperature was observed when the resistor was heated by a 2 mA DC current. The resistance graph follows the same shape as the ambient temperature over time, as seen in Figure 6, and it increases linearly with temperature like in the unheated wire case. The relative humidity of this case is 70%.

Equation (6) can be used to calculate the temperature of the wire since the resistance of the heated wire is known:

$$T_{\text{wire}} = \frac{R_{\text{heated}} - 593.932}{1.2867} \tag{7}$$

Since T_{wire} is the sum of ΔT and T_{ambient}, $\Delta \text{T} = T_{\text{wire}} - T_{\text{ambient}}$ is calculated and used in Equation (4). The entire step-by-step derivation can be found in Appendix C.1.

The values of the used constants are stated in Table 1. Since the shape of the V-groove is unconventional the effective depth is unknown. It is assumed that (d_{eff}) equal to half the distance between the wire and the bottom of the groove describes the heat dissipation properly, but it was fine-tuned to fit the values obtained from the experiment to the values extracted from Figure 3. It was concluded that $d_{\text{eff}} \approx 0.65 \cdot$d.

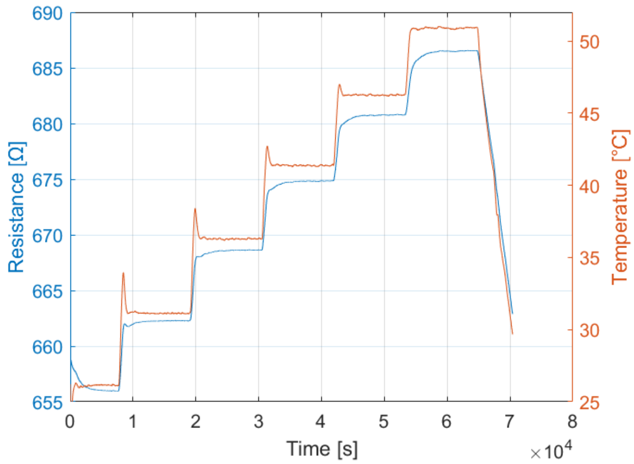

Figure 6: Resistance and ambient temperature when a current of 2 mA is applied at RH=70%.

Constant	A [m^2]	d_{eff} [m]	I^2 [A^2]
Value	1.6e-7	3.6721e-5	4e-6

Table 1: Used constant values for Equation (4)

In Figure 7 it can be seen that ΔT is decreasing as the ambient temperature increases. This will lead to a similar outcome as seen in Figure 3 since resistance is linearly increasing and ΔT is in the denominator of Equation (4).

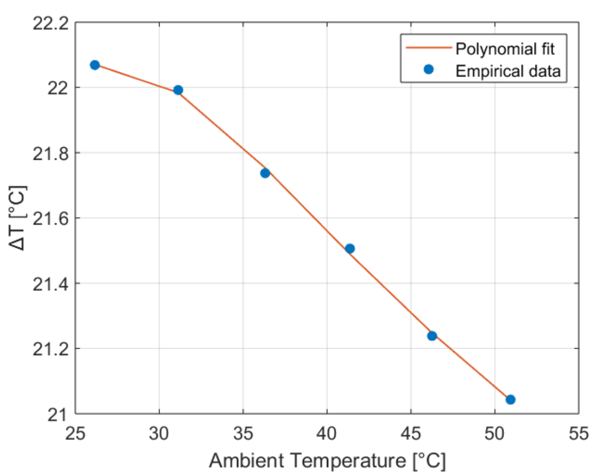

Figure 7: ΔT at different ambient temperatures for RH=70%.

The sensitivity of ΔT on errors must be considered since small resistance changes can completely change the polynomial fit, therefore it will change k's graph. The resistance at an ambient temperature of 41.3634 °C was measured to be 674.8259 Ω. If the true resistance is 675 Ω, i.e. there is an error of 0.026% between the real value and the measured one, the corresponding ΔT increases by almost 0.2 °C, i.e. 20% of the entire range of change in ΔT, and changes the shape of the polynomial fit. A comparison can be found in Appendix B.2.

The thermal conductivity of air for different temperatures at RH=70% was calculated and plotted aside to the theoretical thermal conductivity values at RH=70% taken from [7] and the values for RH=0% in Figure 8. The RH= 0% values were taken from the FLUIDAT database [8]. It must be mentioned that other databases have different values for the same temperature and pressure. The pressure inside the climate chamber is on average 100.7 kPa and the recorded changes fall into the ±0.3 kPa margin which doesn't affect the k from FLUIDAT.

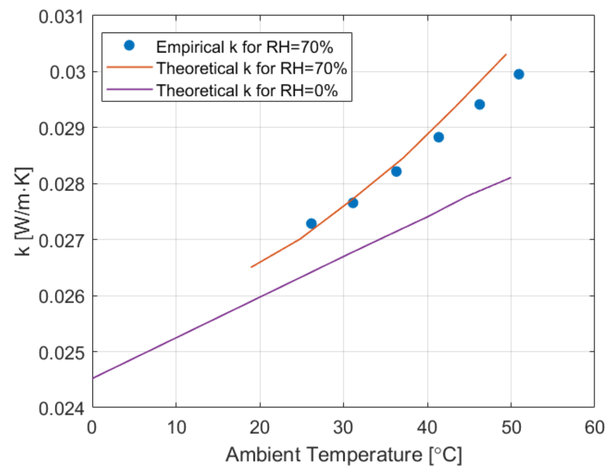

Figure 8: Comparison between empirically obtained values, theoretical ones taken from Figure 3 for RH=70% and FLUIDAT values at RH=0%.

The shape of the plot and the values are similar to the ones in Figure 3. Due to the mismatch of R and ΔT, the values are not the same, but it shows that as the humidity increases, the air's thermal conductivity also increases.

Figure 9 shows the empirically obtained thermal conductivity plots for different humidities.

It cannot be concluded that a higher relative humidity percentage results in a higher k just like in Figure 3. Figure 9 highlights the need for high precision in measurements and confirms that the thermal conductivity increases with the ambient temperature.

4 VOLUMETRIC HEAT CAPACITY

4.1 Literature review

Boukhriss et al. [6] showed that as long as the air is humid the specific heat capacity of air will increase with temperature, and the increase will be faster if the RH percentage is higher. For RH=0% the specific heat capacity is hardly influenced by the ambient temperature. This can be seen in Figure 10.

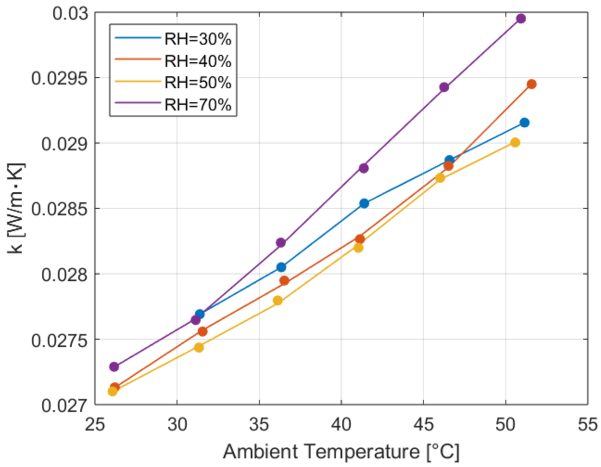

Figure 9: Thermal conductivity obtained experimentally as a function of temperature for different relative humidity percentages.

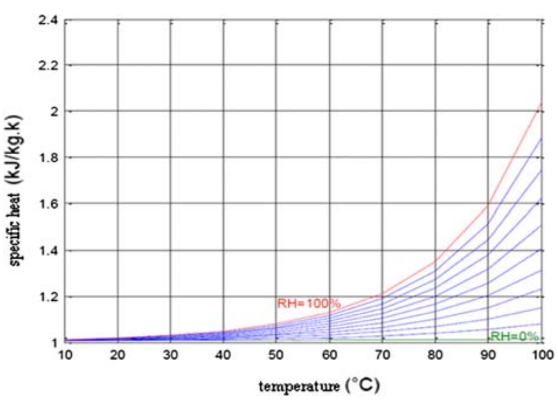

Figure 10: Specific heat capacity as a function of ambient temperature for various relative humidity percentages. Image taken from [6].

The graph of the volumetric heat capacity is more complex since it depends on the rates at which the air's density decreases and specific heat increases. In Figure 11 the graph of air density as a function of ambient temperature for different RH percentages is seen.

For RH=100% the slope of the density between 20 and 30 °C was calculated to be -0.005 [kg/(m^3·°C)], having an absolute value greater than the one of the slope of the specific heat capacity at the same temperatures, i.e. 0.001 [kJ/(kg·K·°C)]. However, at higher temperatures, e.g. 90 and 100°C the slopes are -0.112 [kg/(m^3·°C)] for density and 0.4 [kJ/(kg·K·°C)] for specific heat. Thus, the specific heat increases faster than the density decreases at high temperatures.

However, for lower humidity levels the volumetric heat capacity seems only to decrease. For 30% RH between 20 and 30 °C the slopes of both density and specific heat were considered the same as the 100% RH situation since they

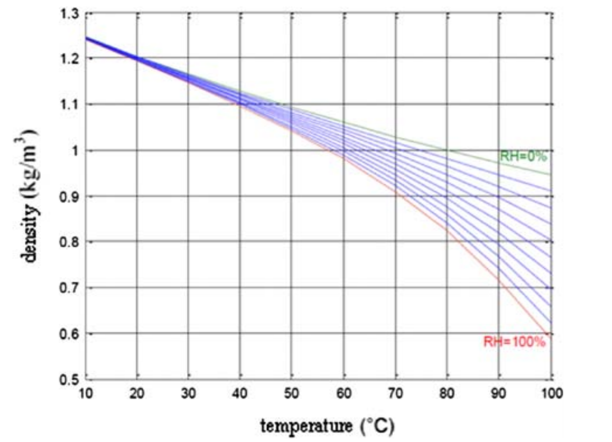

Figure 11: Density as a function of ambient temperature for various relative humidity percentages. Image taken from [6].

could not be differentiated, so the volumetric heat capacity decreases at low temperatures. At 90 and 100 °C for RH=30% the magnitude of the specific heat's slope, equal to 0.0035 [kJ/(kg·K·°C)], proved to be lower than the one of the density, equal to -0.008 [kg/(m^3·°C)], contrary to the previous result at 100% RH.

4.2 Experimental setup

A Howland current pump was designed and realised to supply a 4 mA$_{pp}$ alternating current. The circuit uses a power supply and an AC voltage to supply any load with a fixed amplitude AC. An LTSpice schematic of the circuit can be found in Figure 12.

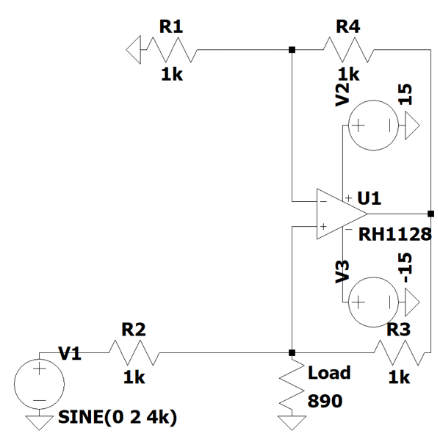

Figure 12: The Howland current pump model in LTSpice, designed for 4 mA peak-peak.

To simplify the calculations, all the resistors except the load were chosen to be 1 kΩ. The resulting current's amplitude through the load equals the AC voltage divided by 1000 Ω, so a 4 V$_{PP}$ leads to 4 mA$_{PP}$. The used Op-Amp is TL071IP but a simulation of the circuit using it could not be made due to the unavailability of the SPICE model. The DC power supply is Agilent E3631A and the AC voltage supply is Agilent 33220A. The current pump proved to perform well, supplying 4 $\mathrm{mA_{PP}}$ for an AC voltage equal to 4.03 $\mathrm{V_{PP}}$ which shows an error of 0.75% for the expected 4 $\mathrm{V_{PP}}$ value. Moreover, the RMS value of the third harmonic was verified on a fixed value resistor of 680 Ω, close to the value of the sensor's wire. The value shown on the lock-in amplifier is 45 μV, i.e. 28 times smaller than the one seen when the sensor uses the same current. The used frequency is 4 kHz because it's higher than the cutoff frequency of the thermal resistance (R_{th}) and capacitance (C_{th}) system [2].

A Stanford Research Systems SR830 lock-in amplifier (LIA) is used to measure the RMS voltage of the third harmonic on the sensor. The data from the LIA is sent to the computer running a Labview program.

4.3 Findings

The third harmonic's RMS value is approximately 1.26 mV at 4 kHz. Due to the small current used and the sensitivity of the LIA, quantisation errors might appear and make the measurement hard to analyse. Moreover, while the SR830 displays R, i.e. the amplitude of the phasor, only the in-phase (X) and the quadrature (Y) components are sent to the computer and then they are used to calculate R = $\sqrt{X^2+Y^2}$. This leads to a slight mismatch of the R displayed on the LIA and the one calculated in Labview, i.e. 0.02 V_{RMS}.

The recorded change in the 3ω component's amplitude is small, in the range of 0.01 mV_{RMS} and does not offer enough information about the temperature's and relative humidity's influence. More than that, it was discovered that what was initially believed to be a quantisation error due to instantaneous jumps between two voltage values proved to be an error of another nature. There are other levels that the voltage could have occupied, yet it did not occur. This is seen in Figure 13, which shows the latest AC experiment conducted. Three cycles can be seen, for 30% RH, 50% RH and 70% RH, each having the same temperature steps but different $V_{3\omega}$(RMS) measurements.

The 25 °C step of the third cycle shows small peaks in the RMS value, proving that there are quantisation levels between the two levels seen in the first cycle at 50 °C. Another inconsistency is seen between the voltage levels of the first and third cycles. If for RH=30% the third harmonic's value seems to increase with the ambient temperature, in the RH=70% case the voltage decreases. The 50% relative humidity case doesn't show any change in the measured voltage, proving even more that the measurement is inconsistent and further investigations are required to evaluate the ambient temperature's and relative humidity's impact on ρc_p.

It was observed that the volumetric heat capacity is directly proportional to the thermal conductivity. The magnitude of $Z_{2\omega}$ present in Equation (5) is:

$$|Z_{2\omega}| = \frac{R_{\text{th}}}{\sqrt{1+4\omega^2 R_{\text{th}}^2 C_{\text{th}}^2}} \tag{8}$$

where C_{th} is the thermal capacitance, parallel to the R_{th} in the

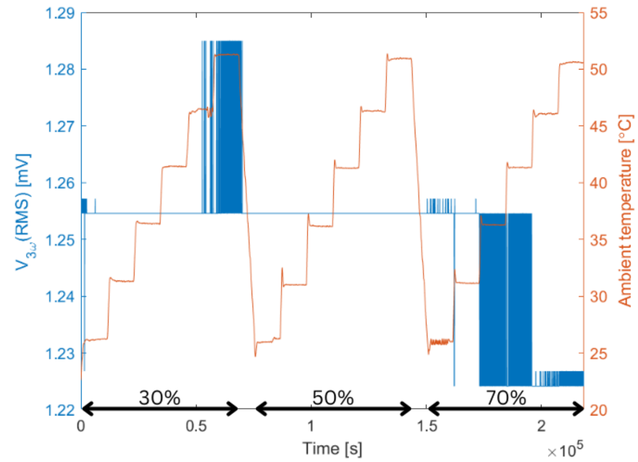

Figure 13: Third harmonic RMS voltage at different ambient temperatures for RH=30% (first cycle), 50% (second cycle), and 70% (third cycle).

thermal domain. The thermal capacitance has the following identity:

$$C_{\text{th}} = \rho c_p \cdot V \tag{9}$$

V is the volume of the V-groove. By rearranging Equation (5) and using Equation (8), C_{th} becomes:

$$C_{\text{th}} = \frac{\sqrt{\left(\frac{R_{\text{th}} I_{\text{ac}}^3 R_{\text{heated}} R_0 \alpha}{4|V_{3\omega}|}\right)^2 - 1}}{2\omega R_{\text{th}}} \tag{10}$$

Since the thermal resistance is

$$R_{\text{th}} = \frac{d_{\text{eff}}}{k \cdot A} \tag{11}$$

i.e. inversely proportional with k, and it's in the denominator of Equation (10), if the measured RMS voltage is constant the volumetric heat capacity will increase with the ambient temperature. The R_{th} under the square root does not influence the C_{th}-k relation as greatly as the one in the denominator. Therefore, it can be concluded that if the third harmonic's magnitude remains constant, the volumetric heat capacity increases with the ambient temperature. However, if another behaviour of $|V_{3\omega}|$ is observed, the influence of temperature and humidity will be more complex.

5 DISCUSSION

The results seem to be similar to the ones that Boukhriss et al. [6] obtained, especially since the decreasing ΔT w.r.t. ambient temperature determines the fast increase in the slopes of thermal conductivity graphs, similar to the ones of Figure 3. However, the measurement errors might drastically affect the calculated thermal conductivity values for different humidities. In Figure 9, the plots for RH=30% and RH=40% are situated above the one for 50% relative humidity. Therefore, the data acquisition requires better measurement equipment with a higher accuracy. The errors can be minimised also by using a smaller climate chamber to easily keep the ambient temperature and relative humidity constant. The Keithley source measure unit's datasheet [9] lists all the accuracies for the current supply and the voltage measurement. For the used channel, the maximum theoretical error of the current supply can lead to a difference of approximately 1.5 Ω between the observed and the true value. This error is almost 10 times bigger than the 0.026% one mentioned in Subsection 3.3. The voltage measurement error is smaller, but it would still impact the outcome of the measurement since the maximum deviation of 0.012% can lead to an error of approximately 0.038% in resistance. Both will lead to significant errors in the thermal conductivity and the volumetric heat capacity.

No volumetric heat capacity graph was found in the literature. However, the sources show very similar graphs in the case of specific heat capacity and the case of density w.r.t. ambient temperature and for different relative humidities, contrary to the thermal conductivity ones. A theoretical volumetric heat capacity graph can be obtained by using the density graph and the specific heat capacity one. In theory, it should decrease for lower humidity levels as the temperature increases, but for higher ones, e.g. RH=100% it should decrease at first and at higher temperatures it increases. Once again, new experiments using better equipment are needed. The problem that was previously believed to be one of a quantisation nature requires more investigation.

6 CONCLUSION

The paper presents an insightful method of measuring the thermal conductivity of humid air and confirms that as the ambient temperature increases the difference between the wire's temperature and the ambient temperature, i.e. ΔT, decreases. This corresponds to an increase in thermal conductivity k as the ambient temperature increases. The relative humidity's impact on the sensor is uncertain due to the need for high-precision resistance measurements. Better measurement equipment can be used to reduce the error and a smaller climate chamber would decrease the run time of the experiments. Small errors in the acquired resistance such as 0.026% can completely change the shape of the thermal conductivity w.r.t. ambient temperature graph.

The volumetric heat capacity measurement did not show promising results, but the method can be used in future experiments after a solution for the lock-in amplifier's errors is found. The measured value of ρc_p is also highly dependent on the k, thus the need for accurate thermal conductivity results is accentuated.

References

[1] S. A. Kenari, R. J. Wiegerink, R. G. Sanders, and J. C. Lötters, "Gas independent thermal flow meter based on real-time velocity-independent k and cp measurement," in *2024 IEEE 37th International Conference on Micro Electro Mechanical Systems (MEMS)*, pp. 801–804, 2024.

[2] S. A. Kenari, R. J. Wiegerink, R. G. P. Sanders, and J. C. Lötters, "Flow-Independent thermal conductivity and volumetric heat capacity measurement of pure gases and binary gas mixtures using a single heated wire," *Micromachines*, vol. 15, p. 671, 5 2024.

[3] S. Emperhoff, M. Eberl, T. Dwertmann, and J. Wöllenstein, "On the Influence of Humidity on a Thermal Conductivity Sensor for the Detection of Hydrogen," *Sensors*, vol. 24, p. 2697, 4 2024.

[4] P. Tsilingiris, "Thermophysical and transport properties of humid air at temperature range between 0 and 100°C," *Energy conversion and management*, vol. 49, pp. 1098–1110, 5 2008.

[5] H.-F. Pernau, M. Benkendorf, M. Jägle, S. Heinrich, T. Knittel, and J. Wöllenstein, "Measuring the thermal conductivity of humid air over a broad temperature and water content range," *Proceedings*, vol. 97, no. 1, 2024.

[6] M. Boukhriss, K. Zhani, and R. Ghribi, "Study of thermophysical properties of a solar desalination system using solar energy," *Desalination and water treatment*, vol. 51, pp. 1290–1295, 1 2013.

[7] Z. Wu, W. Li, H. Tang, S. Luo, and L. Zhang, "Research on the calculation of Rotor's convective heat transfer coefficient of High-Speed Drive Motor for EVs based on multiple scenarios," *Journal of Electrical Engineering Technology/Journal of electrical engineering technology*, vol. 18, pp. 4245–4256, 7 2023.

[8] "FLUIDAT® on the Net, mass flow and physical properties calculations." https://www.fluidat.com/default.asp.

[9] "Series 2400 SourceMeter SMU Instruments Datasheet." https://www.farnell.com/datasheets/3775978.pdf.

Appendix

A AI disclosure

During the preparation of this work, the author used Grammarly to conduct a final spelling/grammar check. After using this tool/service, the author reviewed and edited the content as needed and takes full responsibility for the content of the work.

B Additional figures

B.1 Thermal conductivity plots

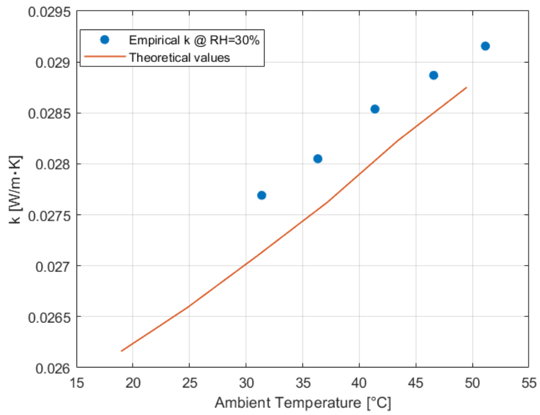

Figure 14: Comparison between empirically obtained values and theoretical ones taken from Figure 3 for RH=30%.

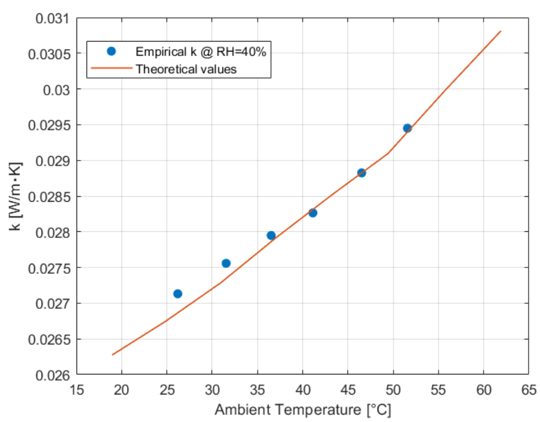

Figure 15: Comparison between empirically obtained values and theoretical ones taken from Figure 3 for RH=40%.

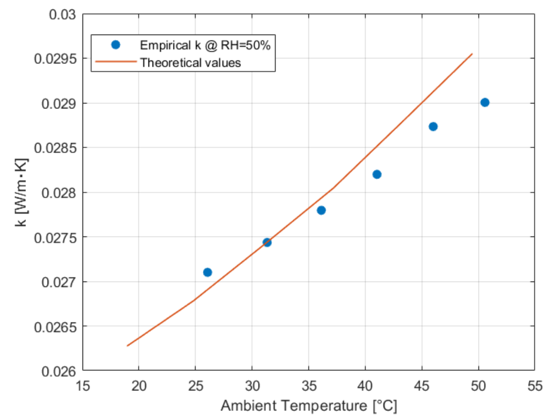

Figure 16: Comparison between empirically obtained values and theoretical ones taken from Figure 3 for RH=50%.

B.2 Errors

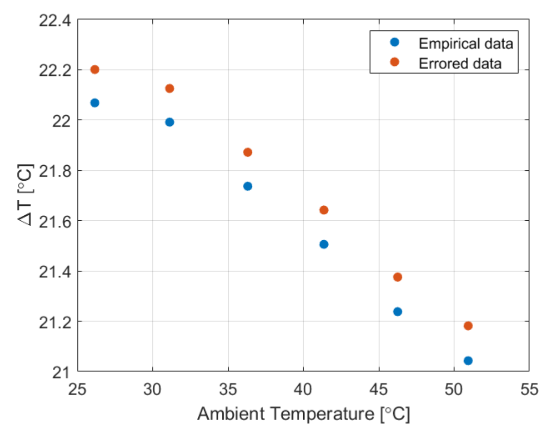

Figure 17: Different ΔT 4th order polynomial fits when one of the resistance values has an error of 0.026%

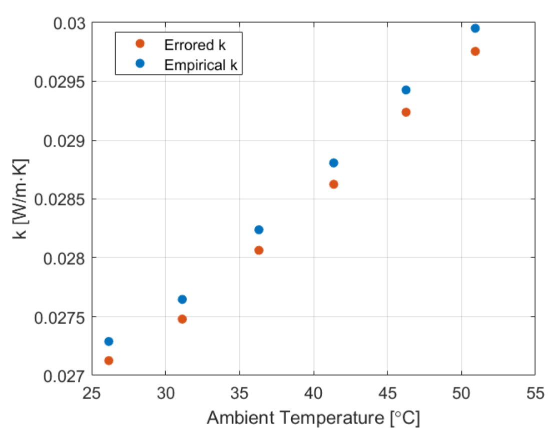

Figure 18: Error in k at 41 °C if the resistance at 2 mA DC has an error of 0.026%

C Experiments workflow

C.1 Thermal conductivity experiment

- **Step 1**: Measure the resistance of the unheated wire using a very small DC current for different ambient temperatures to calculate $R_{\text{unheated},0^\circ\text{C}}$ and the slope.

- **Step 2**: Measure the resistance of the heated wire using a DC current (I_{DC}) for different ambient temperatures.

- **Step 3**: Calculate the wire's temperature using:

$$T_{\text{wire}} = \frac{R_{\text{heated}} - R_{\text{unheated},0^\circ\text{C}}}{\text{slope}}$$

- **Step 4**: Calculate $\Delta T = T_{\text{wire}} - T_{\text{ambient}}$.

- **Step 5**: Calculate the thermal conductivity using:

$$k = \frac{R_{\text{heated}} \cdot I_{\text{DC}}^2 \cdot d_{\text{eff}}}{\Delta T \cdot A}$$

  where d_{eff} is the effective depth of the V-groove and A is the area of the V-groove seen from above.

C.2 Volumetric heat capacity experiment

Note: To calculate ρc_p the thermal conductivity experiment must be conducted since the following parameters will be used in the equation: R_{heated}, R_0, and α.

- **Step 1**: Measure the third harmonic's RMS magnitude ($|V_{3\omega}|$) for an AC current of amplitude I_{ac} and angular frequency ω that is higher than the cutoff frequency of the sensor for different ambient temperatures.

- **Step 2**: Calculate C_{th} using the following equation:

$$C_{\text{th}} = \frac{\sqrt{\left(\frac{R_{\text{th}} I_{\text{ac}}^3 R_{\text{heated}} R_0 \alpha}{4|V_{3\omega}|}\right)^2 - 1}}{2\omega R_{\text{th}}}$$

- **Step 3**: Calculate ρc_p using:

$$\rho c_p = \frac{C_{\text{th}}}{V}$$

  where V is the volume of the V-groove.

D MATLAB and CSV files

.csv file	.mlx file	Description
measurement_unheated.csv	measurement_unheated.mlx	Files for the 100 μA DC measurement
measurement30RH.csv	measurement30RH.mlx	Files for the 2 mA DC measurement at different temperatures and 30% RH
measurement40RH.csv	measurement40RH.mlx	Files for the 2 mA DC measurement at different temperatures and 40% RH
measurement50RH.csv	measurement50RH.mlx	Files for the 2 mA DC measurement at different temperatures and 50% RH
measurement70RH.csv	measurement70RH.mlx	Files for the 2 mA DC measurement at different temperatures and 70% RH
measurementAC.csv	measurementAC.mlx	Files for the 2 mA_{PP} AC measurement at different temperatures and RH levels
N/A	theory.mlx	.mlx file with the k values extracted from literature and theoretically calculated ΔT values